Dynamically hidden reaction paths in the reaction of CF3^+ + CO

Oda, Kohei
Graduate School of Chemical Sciences and Engineering, Hokkaido University

Tsutsumi, Takuro
Department of Chemistry, Faculty of Science, Hokkaido University

Keshavamurthy, Srihari
Department of Chemistry, Faculty of Science, Hokkaido University

Furuya, Kenji
Faculty of Arts and Science, Kyushu University

他

出版情報：ACS Physical Chemistry Au, 2022-04-27. American Chemical Society
バージョン：

Supporting Information

Dynamically hidden reaction paths in the reaction of $CF_3^+ + CO$

Kohei Oda,[a] Takuro Tsutsumi,[b] Srihari Keshavamurthy,[b,c] Kenji Furuya,[d,e,f *] P. B. Armentrout,[f] and Tetsuya Taketsugu[b,g *]

[a] *Graduate School of Chemical Sciences and Engineering, Hokkaido University, Sapporo 060-0810, Japan*

[b] *Department of Chemistry, Faculty of Science, Hokkaido University, Sapporo 060-0810, Japan*

[c] *Department of Chemistry, Indian Institute of Technology, Kanpur 208 016, India*

[d] *Faculty of Arts and Science, Kyushu University, Motooka, Fukuoka 819-0395, Japan*

[e] *Department of Molecular and Material Sciences, Kyushu University, Kasuga, Fukuoka 816-8580, Japan*

[f] *Department of Chemistry, University of Utah, Salt Lake City 84112, U.S.A.*

[g] *Institute for Chemical Reaction Design and Discovery (WPI-ICReDD), Hokkaido University, Sapporo 001-0021, Japan*

S-1. Comparison of relative energies of stationary points in low energy region between UB3LYP and CCSD(T)

Table S1. Relative energies of the stationary points in the low energy region of CF_3^+/CO collision reaction calculated at the levels of CCSD(T)/aug-cc-pVTZ and UB3LYP with several basis sets. The root-mean-square errors (RMSE) in energies compared to the results of CCSD(T)/aug-cc-pVTZ calculations are also shown. The CCSD(T) computations were carried out by Molpro 2012. [1]

	Relative energies / eV				
		UB3LYP with different basis sets			
Structures	CCSD(T)/aug-cc-pVTZ	6-31G(d)	6-31+G(d)	6-311G(d)	6-311+G(d)
Reactants	0	0	0	0	0
I_{CC}	-0.807	-0.840	-0.807	-0.719	-0.742
I_{CO}	-0.349	-0.377	-0.305	-0.325	-0.294
$TS1_{CC}$	0.965	0.651	0.710	0.835	0.816
$I1_{CC}$	0.113	-0.188	-0.137	-0.028	-0.061
P_{FCO+}	2.44	2.60	2.35	2.45	2.31
$TS2_{CC}$	2.14	1.87	1.94	2.09	2.09
TS_{CO}	2.67	2.43	2.55	2.81	2.83
I2	1.23	0.982	1.04	1.15	1.16
P_{CF+}	2.30	2.49	2.30	2.48	2.35
RMSE / eV	-	0.211	0.151	0.104	0.107

Because CCSD(T) is a single-reference theory, it becomes less accurate for electronic states with large multiconfiguration character. Therefore, we checked the CCSD T1 diagnostic values for each of the equilibrium and transition state structures listed in the table to determine how large the multiconfiguration character is. Most of the structures showed a value of less than 0.02, which is the empirical threshold value where the single reference theory can be applied.[2] Only CF^+ showed a value of 0.021, which is slightly above the threshold value. This magnitude is acceptable, however, and we believe that the overall picture of the potential surface obtained by DFT or CCSD(T) is reliable.

S-2. On-the-fly MD simulations with initial relative orientations varied from sudden complex

In the on-the-fly molecular dynamics (MD) simulations, the collision reaction of CF_3^+ + CO is assumed to occur when the reactant molecules collide with the same relative orientation as the structure in TS. Therefore, the initial relative orientation of the reactant molecules was fixed to be the same as that of the sudden complex structure, and the initial velocity was varied by changing the collision angle. Here, we have tested this assumption by calculating the classical trajectories, where the initial relative orientations change from the sudden complex. The $F_3C^{+\cdots}CO$ collisions, the collision angles θ = 60° and 70° were chosen, and the initial coordinates were slightly modified; CF_3^+ and CO were rotated in 30° increments from -90° to 90° around the center-of-mass point in the C_s symmetry plane to change their relative orientations. The angles of these rotations are denoted by $\theta_{\mathrm{CF3+}}$ and θ_{CO}. When both rotation angles are zero, the relative orientation is the same as the orientation of the sudden complex, and the initial coordinates are the same as in the simulation shown in section 4.2. The larger the rotation angle, the larger the relative orientation will be shifted from the orientation of the sudden complex. For each collision angle, four different collision energies of 3, 5, 7, and 10 eV were given along the collision mode in the same way as in the simulations presented in section 4.2.

Figure S1 shows the trajectories run under each initial condition, classified by destination. As in Figure 4(a), it can be seen that the larger the collision energy, the more reactive the trajectory. In other words, the larger the collision energy, the smaller the relative misorientation, and the more reactive the trajectory. In any case, the reactive trajectory is obtained near $\theta_{\mathrm{CF3+}} = \theta_{\mathrm{CO}} = 0$. At collision energy of 3 eV, the reactive trajectories result from a relative orientation that is slightly different from the sudden complex. This may be the result of reorientation due to electrostatic interactions as the reactants approach $TS1_{CC}$, offsetting the initial relative misorientation. The above simulations of $F_3C^{+\cdots}CO$ collisions seem to guarantee the validity of our assumption; we have not performed such simulations for $F_3C^{+\cdots}OC$ collisions, but we assume that similar results will be obtained.

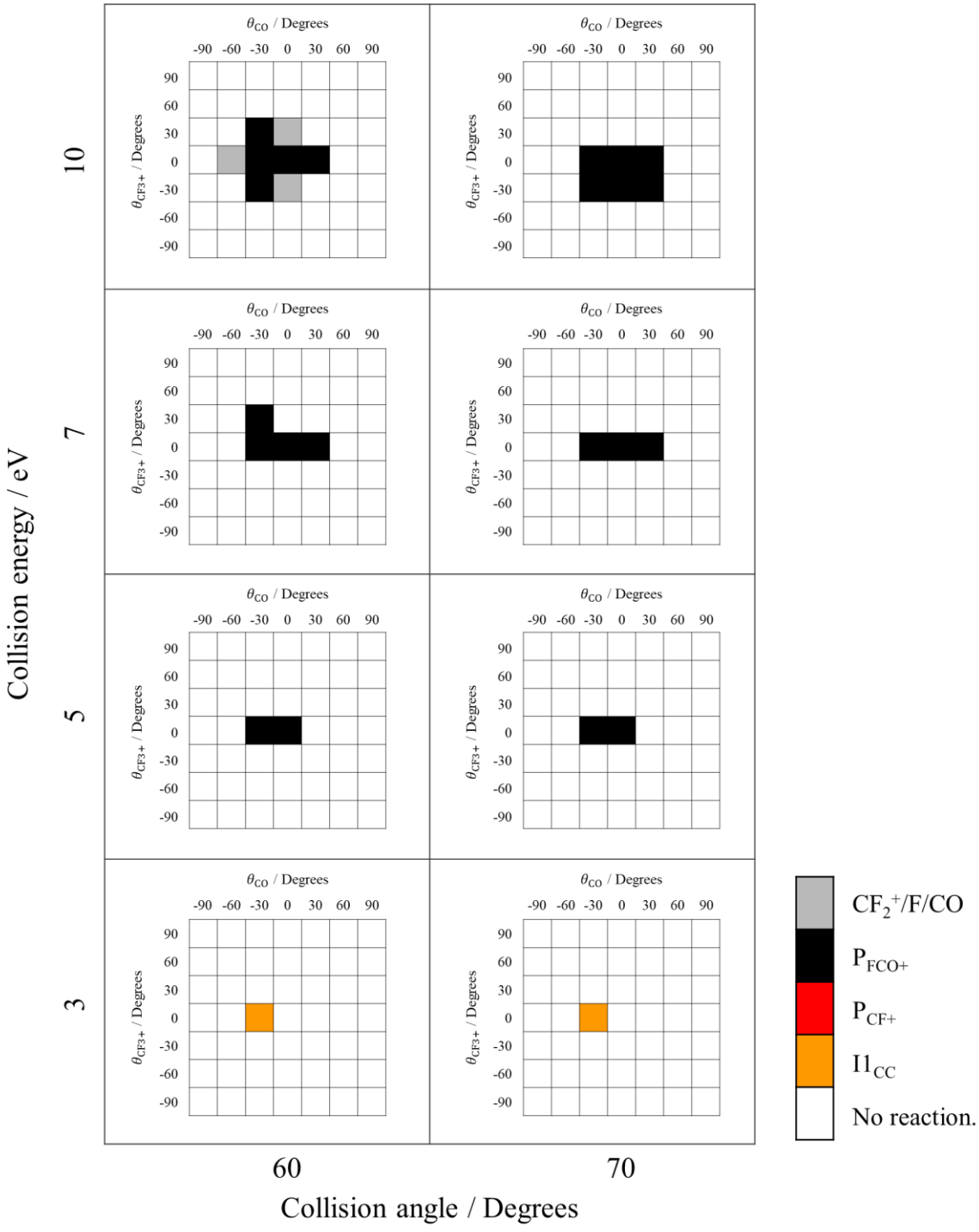

Figure S1. Heatmap of the trajectory termination structure of $F_3C^{+\cdots}CO$ collisions when the initial relative orientation of the reactant molecules is varied. Trajectories assigned to $I1_{CC}$ were trapped around the $I1_{CC}$ structure until 2 ps. For the other trajectories, the molecular system had dissociated within 2ps. No reaction meant that the reacting molecules were scattered.

S-3. Coupling of the collision mode and normal modes at the transition state

The sudden vector projection (SVP) model calculates the contribution of the normal mode of the reactant to the occurrence of the bimolecular reaction based on the SVP value η, which is the inner product of the translational, rotational, and vibrational modes of the reactant and the reaction-coordinate mode at the transition state (TS). In other words, the SVP value can be considered as the expansion coefficient of the reaction-coordinate mode $\mathbf{L}_{\mathrm{RC}}$ projected by the normal mode of the reactants. In this context, $\mathbf{L}_{\mathrm{RC}}$ can be expressed as follows

$$\mathbf{L}_{\mathrm{RC}} = \sum_i \eta_i \mathbf{L}_i \tag{1}$$

where $\eta_i = \mathbf{L}_i \cdot \mathbf{L}_{\mathrm{RC}}$ and $\mathbf{L}_i$ is the normalized basis vector for *the translational, rotational, and vibrational modes of the reactant molecules*. Since the reaction-coordinate mode is defined at TS, the SVP value is meaningful only for the relative orientation of reactants close to the TS structure. Therefore, this SVP analysis must be performed for the sudden complex structure; the normal mode with the largest absolute value of η corresponds to the most efficient reaction mode.

We now introduce an SVP-like analysis in which the intermolecular collision mode of the reactants is expanded by the modes at TS as follows

$$\mathbf{L}_{\mathrm{coll}}(\theta) = \sum_i \eta'_i(\theta) \mathbf{L}_i \tag{2}$$

where θ represents the collision angle, $\eta'_i(\theta) = \mathbf{L}_i \cdot \mathbf{L}_{\mathrm{coll}}(\theta)$, and $\mathbf{L}_i$ represents *the reaction-coordinate mode, rotation mode, and vibration mode at TS*. Based on the above expansion equation, the collision momentum $\mathbf{P}_{\mathrm{coll}}$ can be decomposed into the momentum along each mode at TS, *i.e.* $\mathbf{P}_i$. $\mathbf{P}_{\mathrm{coll}}$ is

$$\mathbf{P}_{\mathrm{coll}} = P_{\mathrm{coll}}\, \mathbf{L}_{\mathrm{coll}} = \sum_i P_{\mathrm{coll}}\, \eta'_i\, \mathbf{L}_i \equiv \sum_i \mathbf{P}_i \tag{3}$$

where P_{coll} denotes the magnitude of the collision momentum, and θ is omitted for simplicity of notation. Following the same approach, the collision energy E_{coll} can be decomposed into the energy E_i along each mode at TS.

$$E_{\mathrm{coll}} = \sum_i E_i \sim \sum_i \frac{\mathbf{P}_i^2}{2}. \quad (4)$$

Since the reaction occurs through the vicinity of the TS and the potential energy terms along each mode at TS are expected to be small compared to the kinetic energy terms, these terms are neglected. Substituting the definition of $\mathbf{P}_i$ shown in Eq. (3) gives

$$E_{\mathrm{coll}} = \sum_i E_i \sim \sum_i \frac{P_{\mathrm{coll}}^2 \eta'^2_i \mathbf{L}_i^2}{2} = \sum_i \frac{P_{\mathrm{coll}}^2 \eta'^2_i}{2}. \quad (5)$$

Here, $P_{\mathrm{coll}}^2/2$ is E_{coll}. Finally, E_{coll} can be seen in terms of the SVP-like values as

$$E_{\mathrm{coll}} = \sum_i E_i \sim \sum_i E_{\mathrm{coll}} \eta'^2_i . \quad (6)$$

The square of the SVP-like value η'_i gives the energy ratio about each mode, estimating the fast energy redistribution occurring with a reactants' collision. However, in the actual chemical reaction process, the collision momentum, which the reactants initially have, changes its direction and magnitude while the molecular system approaches the TS due to the shape of the PES. Therefore, the analysis gives qualitative or semi-quantitative results.

S-4. On-the-fly MD simulations with zero-point vibrational energies

We carried out on-the-fly MD simulations for CF_3^+/CO collision reactions with the collision energies below 5 eV, including the motions in all degrees of freedom. Zero-point vibrational energies were added to SVP-based initial conditions as velocities and structural deviations of each reactant with random phases, and collision angles were set to 60° and 70°. The trajectory calculation was stopped when the C···C distance was greater than 6 Å within 2 ps. Five of the trajectories which went back to the reactants had the convergence problem in the electronic structure calculations before they met the dissociation criterion. Thus we assigned these trajectories manually to each channel based on the molecular geometry at that point. **Table S2** shows destinations of 600 trajectories, and some trajectories lead to P_{FCO+} but no trajectories to P_{CF+}. Among them, only one trajectory does not undergo dissociation

within 2 ps after crossing $TS1_{CC,}$ and the molecular system remains trapped in the $I1_{CC}$ region. This result suggests the possibility that a small fraction of the initial conditionscan stay trapped at $I1_{CC}$ under a statistical distribution among all the degrees of freedom due to an intramolecular vibrational-energy redistribution. Then, it is valuable to estimate the reaction rate constants for the elementary processes starting from this minimum.

Table S2. Distributions of the number of trajectories classified by several destinations (reactants, dissociation channels, and intermediate).

Initial conditions		Reactants	P_{FCO+}	P_{CF+}	$I1_{CC}$	Total
E_{coll} / eV	θ / deg	CF_3^+/CO	FCO^+/CF_2	CF^+/F_2CO	F_2CCFO^+	
5	60	27	73	0	0	100
	70	27	73	0	0	100
4	60	94	5	0	1	100
	70	92	8	0	0	100
3	60	100	0	0	0	100
	70	100	0	0	0	100

Here, we assume a microcanonical ensemble for $I1_{CC}$ and calculate the rate constants for the reverse reaction to the reactants through $TS1_{CC}$ and the further reaction to $I2_{CC}$ through $TS2_{CC}$ by employing the Rice-Ramsperger-Kassel-Marcus (RRKM) theory. When the total energy of the system is 2.35 eV that is sufficient to produce P_{FCO+} (including no zero-point vibrational energies), the total energy is higher than the barrier heights for $TS1_{CC}$ and $TS2_{CC}$, and thus, we use RRKM rate constants in the classical limit

$$k_{\mathrm{cl}} = \left(\frac{E - E_{\mathrm{act}}}{E}\right)^{s-1} \frac{\prod_{i=1}^{s} c\tilde{\nu}_i}{\prod_{i=1}^{s-1} c\tilde{\nu}_i^{\ddagger}} \tag{7}$$

where E is the total energy, E_{act} is the activation barrier, s (= 12) is the numbers of vibrational degrees of freedom, c is the speed of light, $\tilde{\nu}_i$ is a vibrational frequency of $\mathrm{I1_{CC}}$, and $\tilde{\nu}_i^{\ddagger}$ is that of the TS. The energies are relative value to $\mathrm{I1_{CC}}$. For example, $E = 2.49$ eV and $E_{\mathrm{act}} = 2.08$ eV for the reaction process *via* $\mathrm{TS2_{CC}}$. The RRKM rate constants for the reverse reaction through $\mathrm{TS1_{CC}}$ and the further reaction through $\mathrm{TS2_{CC}}$ are 31 $\mathrm{ns^{-1}}$ and 2.0×10^{-5} $\mathrm{ns^{-1}}$, respectively, suggesting a much greater possibility of crossing $\mathrm{TS1_{CC}}$ than crossing $\mathrm{TS2_{CC}}$. **Table S3** shows the vibrational frequencies of $\mathrm{I1_{CC}}$, $\mathrm{TS1_{CC}}$, and $\mathrm{TS2_{CC}}$ used in the rate constant calculation.

Table S3. Vibrational frequencies of $\mathrm{I1_{CC}}$, $\mathrm{TS1_{CC}}$, and $\mathrm{TS2_{CC}}$. The imaginary frequencies of the reaction-coordinate mode are not used in the rate constant calculations.

Frequencies / $\mathrm{cm^{-1}}$		
$\mathrm{I1_{CC}}$	$\mathrm{TS1_{CC}}$	$\mathrm{TS2_{CC}}$
31	496*i*	594*i*
213	173	94
377	308	201
416	337	358
494	490	484
654	591	554
775	632	660
782	795	893
1185	851	1047
1461	1423	1423
1612	1530	1532
1930	2245	1589

S-5. On the fly MD from a TS to reactants

Although it is not mentioned in our manuscript, we also performed on-the-fly MD simulations from the transition states, $TS2_{CC}$ and TS_{CO}, toward the reactant side. This is a typical way to examine the energy distribution among the reactants in order to reach the TS, taking into account the time-reversal symmetry of Newton's equations of motion. Although the simulations from a TS to reactants do not represent the molecular system in the GIB experiment, it can be said that it is difficult to reach $TS2_{CC}$ or TS_{CO} only with the translational energy just above their barrier heights. Actually, the time-reversal simulation results showed large rovibrational energies in the reactants, which rarely exist in the experiment, in addition to the translational energy. When the molecular system has the total energy just above these barrier heights, a substantial contribution from rovibrational energies is required to reach these TSs. Details are shown below.

As an initial condition, kinetic energy of 0.1 eV is given along the reaction-coordinate mode towards the reactant side at each TS. Once the molecular system reaches the reactant region (when the C-C interatomic distance reaches 9 Å), the translational and rotational energies were calculated from the mean value of the kinetic energy for the time range where the C-C interatomic distance is between 6 and 9 Å, while the vibrational energy was evaluated from twice the mean value of the kinetic energy for the same time range, which is validated by the virial theorem for a harmonic oscillator. The trajectory starting from $TS2_{CC}$ was trapped for about 2.2 ps around the $I1_{CC}$ minimum. After that, it got over $TS1_{CC}$ and reached the reactant region at about 2.5 ps. On the other hand, the trajectory starting from TS_{CO} rapidly dissociated into the reactants. **Figure S2** shows the time evolutions of the kinetic energy decomposed into translational, rotational, and vibrational motions of the reactants along the trajectories. The energy decomposition analysis shows that the translational, rotational, and vibrational energies of the reactant molecules from $TS2_{CC}$ are 0.52, 0.58, and 0.93 eV, respectively, while the corresponding energies of the reactant molecules from TS_{CO} are found to be 1.6, 0.78, and 0.26 eV, respectively. In both cases, excessively large energy is needed in the rotational or vibrational mode to reach the

corresponding transition state. In the GIB experiments, the translational energy can be tuned, but the rotational and vibrational energies follow a Boltzmann distribution at room temperature, so the probability of reactant molecules reaching the $TS2_{CC}$ or TS_{CO} region by following these pathways is very low.

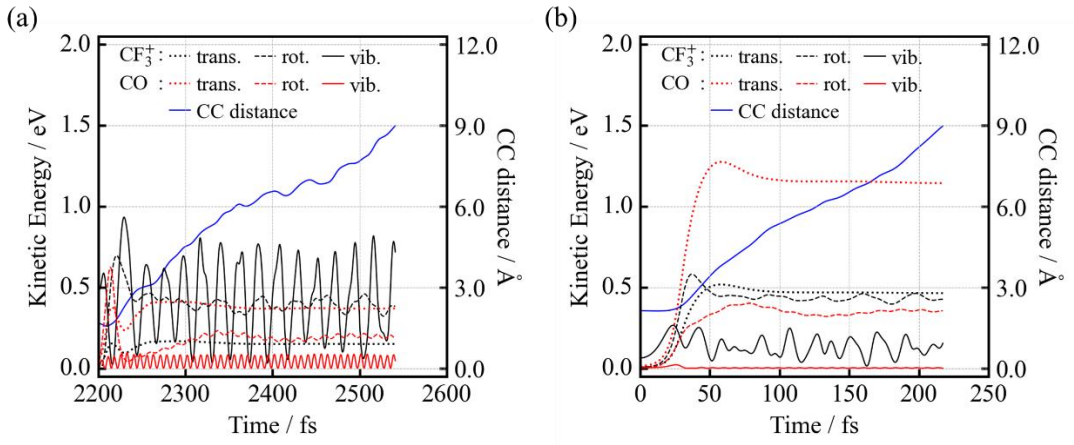

Figure S2. The time evolutions of the kinetic energies decomposed to the degrees of freedom and C-C interatomic distance for (a) the trajectory from $TS2_{CC}$ toward reactant side and (b) the trajectory from TS_{CO} toward reactant side, along the respective trajectories.

Related to Figure S2, we would like to comment on the well-known charge delocalization error in density functional theory. In the dynamics simulation of the CF_3^+ + CO collision reaction, the positive charge is localized to the CF_3 site in the reactant region, which is well described, but in the product region, the positive charge is delocalized to some extent, which is not a very good description. In the trajectory in Figure 4(b), the FCO moiety had a charge of +0.98 at 200.0 fs, +0.90 at 248.0 fs, and +0.84 at 313.2 fs. In the trajectory in Figure 5(b), the CF^+ portion had a charge of +0.77 at 100.0 fs, +0.91 at 150.0 fs, and +0.67 at 198.8 fs. Because of this delocalization of charge on the product side, it would seem that the error in the Coulomb interaction between the products would also be large in our trajectory,

but the effect would be small for the branching to dissociated products. This is because the charge distribution is well described from the reactant side to the transition state resulting from collisions. The constant translational energy of well-separated CF_3^+ and CO on the reactant side, as shown in Figure S2, is clear evidence that the charge distribution is accurately described. If delocalization errors do occur, one would expect the translational energies to gradually increase as the reactant molecules move away from each other.

S-6. Cartesian coordinates of transition state structures and sudden complex structures (in Å)

$TS1_{CC}$

C	-0.460474	0.316644	0.000000
F	0.038041	-1.332144	0.000000
F	-1.064116	0.566071	1.080518
F	-1.064116	0.566071	-1.080518
C	0.965689	-0.046728	0.000000
O	2.103651	0.035057	0.000000

$TS2_{CC}$

C	-0.724417	0.334725	0.000000
F	2.154862	-0.870308	0.000000
F	-1.377598	0.329442	1.069765
F	-1.377598	0.329442	-1.069765
C	0.900247	-0.776311	0.000000
O	0.581149	0.582419	0.000000

TS_{CO}

C	-0.309763	0.355640	0.000000
F	0.168841	-1.330316	0.000000
F	-0.924763	0.552841	1.077153
F	-0.924763	0.552841	-1.077153
C	1.550373	-0.697630	0.000000

O	1.065527	0.523389	0.000000

Sudden complex for $TS1_{CC}$

C	-0.655504	0.000104	-0.000016
F	-0.030840	-1.076136	0.000011
F	-0.968079	0.538027	1.077636
F	-0.968085	0.538043	-1.077637
C	0.969279	-0.046470	0.000000
O	2.100958	0.034864	0.000000

Sudden complex for TS_{CO}

C	-0.516531	0.000104	-0.000016
F	0.108216	-1.076088	0.000011
F	-0.829147	0.538003	1.077636
F	-0.829153	0.538019	-1.077637
C	1.512595	-0.602492	0.000000
O	1.093869	0.452013	0.000000

References

(1) MOLPRO, version 2012.1, is a package of ab initio programs written by H.-J. Werner, P. J. Knowles, G. Knizia, F. R. Manby, M. Schütz, P. Celani, W. Györffy, D. Kats, T. Korona, R. Lindh, A. Mitrushenkov, G. Rauhut, K. R. Shamasundar, T. B. Adler, R. D. Amos, S. J. Bennie, A. Bernhardsson, A. Berning, D. L. Cooper, M. J. O. Deegan, A. J. Dobbyn, F. Eckert, E. Goll, C. Hampel, A. Hesselmann, G. Hetzer, T. Hrenar, G. Jansen, C. Köppl, S. J. R. Lee, Y. Liu, A. W. Lloyd, Q. Ma, R. A. Mata, A. J. May, S. J. McNicholas, W. Meyer, M. E. Mura, A. Nicklaß, D. P. O'Neill, P. Palmieri, D. Peng, K. Pflüger, R. Pitzer, M. Reiher, T. Shiozaki, H. Stoll, A. J. Stone, R. Tarroni, T. Thorsteinsson, M. Wang, M. Welborn, see http://www.molpro.net (accessed date 9 March, 2021)

(2) T. J. Lee and P. R. Taylor, *Int. J. Quantum Chem.*, 1989, **36**, 199-207